applied sciences

MDPI

Article

# A Study on the Effects of Vertical Mass Irregularity on Seismic Behavior of BRBFs and CBFs

**Armin Karami [1], Shahrokh Shahbazi [2] and Mahdi Kioumarsi [3,*]**

[1] Department of Civil, Environmental and Land Management Engineering, Politecnico di Milano University, 20133 Milan, Italy; armin.karami@mail.polimi.it
[2] Department of Civil Engineering, Ghiassedin Jamshid Kashani University, Qazvin 34413-56611, Iran; shahrokh.shahbazi25@yahoo.com
[3] Department of Civil Engineering and Energy Technology Civil Engineering, OsloMet–Oslo Metropolitan University, 0166 Oslo, Norway
* Correspondence: mahdik@oslomet.no; Tel.: +47-6723-8745

Received: 22 October 2020; Accepted: 20 November 2020; Published: 24 November 2020


**Abstract:** Today, architectural application and economic constraints require that vertical-irregular structures be constructed in urban areas. Proposing methods to minimize damage to these structures during earthquakes is therefore crucial. Strict regulations have been enforced for the design and analysis of irregular structures given their higher vulnerability to damage compared to that of regular structures. The present study aimed to evaluate eight regular and irregular 10-story and 15-story steel structures with buckling-restrained braces frames (BRBFs) and concentric braced frames (CBFs) in terms of their responses to twelve far-field earthquakes. According to the obtained results, the mean value of maximum drift, top floor displacement and floor acceleration were higher in both regular and irregular structures with BRBFs than in those with CBFs.

**Keywords:** buckling resistant braced frames (BRBFs); vertical irregularity; mass irregularity; far-field earthquake

## 1. Introduction

Buckling restrained braces (BRBs) are seismic elements that comprise an axially yielding core and an axially decoupled restraining mechanism, which suppress the overall buckling. BRBs generally comprise of a mortar-filled steel section that encloses a yielding core wrapped in a thin debonding layer or gap between the core and mortar or all-steel restrainer. As a low-friction interface, this layer limits the axial load transferred to the restrainer in BRBs through accommodating the core lateral expansion caused by the Poisson impact [1]. Given the significant energy dissipation capacity of BRBs compared to that of other completely ductile systems, properly designed BRBs could serve as hysteretic dampers with adequate fatigue capacity for safely withstanding earthquakes of different magnitudes without suffering noticeable damage [1]. In 2017, Takeuchi and Wada proposed the main criteria for the modern design of BRBs and discussed their applications in high-rise buildings [2].

Numerous seismic resistant members employed to decrease the probability of structural collapse during earthquakes include concrete-filled steel tubes, shear walls, braces and structures confined with high-strength concrete [3–9]. Given their significantly higher seismic performance compared to that of conventional braced frames (CBFs), buckling-restrained braced frames (BRBFs) are growingly used today as efficient seismic load resistant frames in regions with high seismic hazard levels. The main difference between these two types of frames lies in the free bucking characteristic of BRBFs [10,11]. Steel BRBFs were also found to significantly increase the energy dissipation capacity, ductility, and hysteretic stability of structures [12].

The seismic performance of buildings can be improved by increasing post-yield energy dissipation and elastic stiffness using BRBFs in their design [13]. Many experimental, numerical, and analytical studies have investigated the incorporation of BRBFs as dampers into the outrigger system [14–22]. Zhou et al. [21] recommended using BRBs as diagonal web members in steel outrigger trusses and found this outrigger configuration to significantly dissipate energy in rare earthquakes.

Torsional and mass irregularity and weak story are among the factors that may result in inaccurate prediction of seismic response of irregular structures. Heavier stories need larger and heavier structural elements, which result in unavoidable stiffness and strength irregularity. Depending on the location of irregularity, appropriate structural models and analytical methods should be used to examine its effects [22]. According to the Iranian code of practice for seismic resistant design of buildings [23], building irregularities involve both height and plan. Vertical irregularities caused by changes in the dynamic properties of structures along their height, e.g., strength, stiffness, and mass, were referred in literature as nongeometric irregularities [24]. A large body of literature is also devoted to the impact of vertical irregularities on the seismic performance of structures [25–29]. Because of the existence of aesthetic consideration and city regulation, irregular configurations, in plan and elevation of buildings, are inevitable. However, these buildings may have to withstand large earthquakes in the future; therefore, their behavior, when subjected to earthquakes, needs to be evaluated. It is believed that vertical irregularities are one of the important causes of structure failures under seismic load. In the past earthquakes, majority of the collapsed structures had irregular distribution of mass. Excess mass might cause rapid increase in lateral inertia forces, ductility reduction in column, and increase of collapse tendency because of P-delta effects [30].

It is worthwhile to note that large structures or high-rise buildings were more affected due to the long duration and narrow band nature of far-field excitation [31]. Resonance phenomenon is the effect occurred when the frequency of ground motion matches the natural frequency of a structure. It will suffer the damage and large oscillations [31]. As a result, in assessment of seismic responses of tall buildings, far-field ground motions should be taken into account.

### *1.1. Literature Review*

Conventional steel braces were initially mounted in steel frames to increase the seismic capacity [32]. Shen et al. [33] reported a higher resistance to earthquake for BRBs compared to that of conventional braces. Hsiao et al. [34], using a novel model, investigated the buckling response of conventional steel braces. Analyzing BRBFs by employing different gaps between core and external sheath, Rafezi and Hoveidae [35] reported the significant effect of bending stiffness of all-steel BRBFs on their global buckling behavior. Mohebbi and Hosseinzadeh [36] found all-steel BRBFs to protect structures under seismic loads within life safety levels by comparing their behavior for different gaps between core and steel casing with that of regular convergent cross bracings. According to Zhu et al. [37], the deformed BRB web can enhance resistance to out-of-plane buckling and raise buckling strength against high quake loads. In contrast to regular steel braces, a novel all-steel BRBF introduced by different researchers [38–41], was found to increase the formability and energy absorbability at a high formability and maintain the performance of tall structures within their service life.

Previous researches suggest that employing the techniques commonly used for regular structures cannot accurately obtain inelastic seismic response of irregular structures and its difference from that of regular structures [42–44]. Furthermore, different analytical methods for irregular structures compared to those applied to regular structures are provided by seismic codes [45]. The equivalent lateral force method is not applicable to analyzing irregular structures, although modal response spectrum analysis, linear response history analysis and nonlinear response history analysis are allowed owing to their use of higher mode effects.

In 2015, Sadjadi and Davoodi [46] explored the effects of far-field earthquakes on the seismic response of single degree of freedom systems considering soil-structure interactions. Numerous studies have also examined the responses of buildings to far-field earthquakes [46–51]. Bento and Belejo [52]

assessed the accuracy of the improved modal pushover analysis for asymmetric plan structures. In addition, Balic et al. [53] modified the multimodal pushover method, and Li et al. [54] appraised the precision of static nonlinear analysis using a tested reinforced concrete frame. Shahbazi et al. [55] studied the seismic behavior of special moment frames (SMFs) with special ductility undergoing near- and far-field earthquakes by considering different modes, including the effects of soil-structure interaction, permanent displacement (Fling step), and forward directivity in near-field earthquake records, as well as vertical component of near-field earthquakes. It was demonstrated that near-field earthquakes impose more damage on the structure than far-field earthquakes [56–58].

Undoubtedly, the existence of vertical irregularities, opting for sort of braces, and the distance of the structure from the active fault, are three important and decisive factors in analyzing the seismic performance of the structures. Hence, in the present study, effects of the aforementioned factors have been evaluated simultaneously.

### *1.2. Objective of the Study*

The present study aims to illustrate a new study into the effect of far-field earthquake in selecting appropriate braces in regular and irregular structures by comprehensively comparing regular and irregular structures with concentric braces and buckling-restrained braces frames (BRBFs) in terms of their seismic behavior. In other words, this study examined the effect of this type of brace on the seismic responses of irregular and regular structures. Nonlinear analyses were performed on four 10-story and four 15-story structures, each group comprising two regular structures with concentric braces and BRBs and two mass-irregular structures with concentric braces and BRBs. A nonlinear time history analysis was conducted on all the structures to compare their seismic responses as well as drift, floor displacement, floor acceleration and base shear. Twelve far-field earthquake records were used to analyze the structures given that their majority were at least 10 km away from the closest active fault.

## 2. Buildings Studied

### *2.1. Design of the Buildings*

In the HAZUS-MH MR5 guidelines [59], buildings with more than eight stories are referred to as high-rise buildings. To assess and compare the seismic behavior of lateral systems, eight 10- and 15-story steel-frame buildings—four regular and four irregular—with CBF and BRBF were chosen to be modeled. Three-dimensional models were designed in accordance with the ACI318-05 [60] in ETABS software. The structures were designed in ETABS using ST37 steel with a yield stress ($F_y$) of 2400 kg/cm$^2$ and an ultimate stress ($F_u$) of 3700 kg/cm$^2$. The dead and live loads of these buildings were 450 (kg/m$^2$) and 200 (kg/m$^2$), respectively. According to the design code [23], when the mass of a building floor exceeds 1.5 times of the mass of the adjacent floors, the building has mass irregularity. On the other hand, there is no agreement about the most effective and critical position of an irregular floor [61]. In the present study, floors with mass irregularities were chosen to be the second and sixth floors in the 10-story building and the second and 12th floors in the 15-story building. Figure 1 shows the position of floors with mass irregularities.

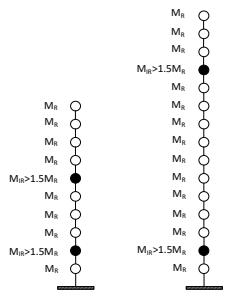


**Figure 1.** Mas irregularity positions in the simulated buildings.

### 2.2. Simulated Frames in OpenSees

An exterior frame was selected as a representative of a three-dimensional structure in two-dimensional analysis. Linear analysis was first performed on the frames to ensure the linear capacity of the structural sections and then calculate the required sections for nonlinear dynamic analysis in OpenSees.

The period of the two-dimensional frames modeled in OpenSees was the same as the vibrational period of the three-dimensional structures designed in ETABS. Tables 1 and 2 illustrate the cross sections of structures frames. The schematic view of the reference frames is shown in Figure 2. In addition, Table 3 presents the fundamental period values of the structures being assessed in the present study.

**Table 1.** Columns and beams cross sections—10-Story frames.

| **Regular Frames** | | | | | **Mass Irregularity Frames** | | | | |
|---|---|---|---|---|---|---|---|---|---|
| **[R-BRBF [1]/R-CBF [2]]** | | | | | **[MIR-BRBF [3]/MIR-CBF [4]]** | | | | |
| Column Sections (width × thickness) (mm) | | | | | Column Sections (width × thickness) (mm) | | | | |
| C1 | C2 | C3 | C4 | C5 | C1 | C2 | C3 | C4 | C5 |
| 250 × 20 | 550 × 40 | 400 × 30 | 550 × 40 | 250 × 20 | 360 × 30 | 550 × 40 | 400 × 30 | 550 × 40 | 360 × 30 |
| C6 | C7 | C8 | C9 | C10 | C6 | C7 | C8 | C9 | C10 |
| 230 × 15 | 500 × 30 | 230 × 15 | 500 × 30 | 230 × 15 | 300 × 25 | 500 × 30 | 350 × 25 | 500 × 30 | 300 × 25 |
| C11 | C12 | C13 | C14 | C15 | C11 | C12 | C13 | C14 | C15 |
| 170 × 12 | 400 × 30 | 300 × 25 | 400 × 30 | 170 × 12 | 280 × 15 | 400 × 30 | 300 × 25 | 400 × 30 | 280 × 15 |
| Beam Sections * (mm) | | | | | Beam Sections * (mm) | | | | |
| B1 | | B2 | | B3 | B1 | | B2 | | B3 |
| IPE270 | | IPE240 | | IPE220 | IPE300 | | IPE270 | | IPE220 |
| * Beam sections were chosen from European standard profiles. | | | | | 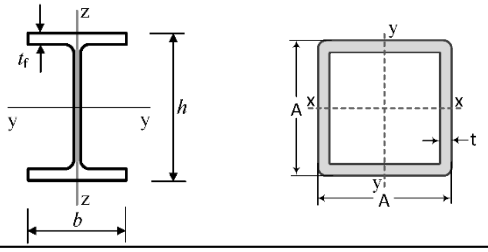 | | | | |
| [1] Regular-Buckling Resistant Braced Frame (R-BRBF)<br>[2] Regular-Concentric Braced Frame (R-CBF)<br>[3] Mass Irregularity-Buckling Resistant Braced Frame (MIR-BRBF)<br>[4] Mass Irregularity-Concentric Braced Frame (MIR-CBF) | | | | | | | | | |

**Table 2.** Columns and beams cross sections—15-Story frames.

| **Regular Frames** | | | | | **Mass Irregularity Frames** | | | | |
|---|---|---|---|---|---|---|---|---|---|
| **[R-BRBF [1]/R-CBF [2]]** | | | | | **[MIR-BRBF [3]/MIR-CBF [4]]** | | | | |
| Column Sections (width × thickness) (mm) | | | | | Column Sections (width × thickness) (mm) | | | | |
| C1 | C2 | C3 | C4 | C5 | C1 | C2 | C3 | C4 | C5 |
| 400 × 30 | 600 × 40 | 400 × 30 | 600 × 40 | 400 × 30 | 400 × 30 | 700 × 60 | 400 × 30 | 700 × 60 | 400 × 30 |
| C6 | C7 | C8 | C9 | C10 | C6 | C7 | C8 | C9 | C10 |
| 360 × 30 | 550 × 40 | 360 × 30 | 550 × 40 | 360 × 30 | 360 × 30 | 550 × 40 | 360 × 30 | 550 × 40 | 360 × 30 |
| C11 | C12 | C13 | C14 | C15 | C11 | C12 | C13 | C14 | C15 |
| 280 × 15 | 500 × 30 | 280 × 15 | 500 × 30 | 280 × 15 | 280 × 15 | 500 × 30 | 280 × 15 | 500 × 30 | 280 × 15 |
| C16 | C17 | C18 | C19 | C20 | C16 | C17 | C18 | C19 | C20 |
| 230 × 15 | 450 × 25 | 230 × 15 | 450 × 25 | 230 × 15 | 230 × 15 | 450 × 25 | 230 × 15 | 450 × 25 | 230 × 15 |
| C21 | C22 | C23 | C24 | C25 | C21 | C22 | C23 | C24 | C25 |
| 174 × 12 | 400 × 20 | 174 × 12 | 400 × 20 | 174 × 12 | 174 × 12 | 400 × 20 | 174 × 12 | 400 × 20 | 174 × 12 |
| Beam Sections (mm) | | | | | Beam Sections (mm) | | | | |
| B1 | | B2 | | B3 | B1 | | B2 | | B3 |
| IPE300 | | IPE270 | | IPE240 | IPE300 | | IPE270 | | IPE240 |

The signals ([1,2,3,4]) have the same meaning in Table 1.


**Figure 2.** (**a**) Plan of structures and (**b**) topology and grouping details of frames.

**Table 3.** Fundamental periods of structures (sec).

| **Regular Buildings** | | | |
|---|---|---|---|
| 10-Story BRBF | 10-Story CBF | 15-Story BRBF | 15-Story CBF |
| 1.15 | 1.057 | 1.58 | 1.654 |
| **Mass Irregularity Buildings** | | | |
| 10-Story BRBF | 10-Story CBF | 15-Story BRBF | 15-Story CBF |
| 1.106 | 1.083 | 1.497 | 1.507 |

### *2.3. Nonlinear Analysis of the Frames*

In OpenSees, material and element are required to be defined nonlinearly to model beam, column, and bracing steel elements. The present study modeled the behavior of steel materials using "*Steel02*" with a yield stress of 2400 kg/cm$^2$, an initial modulus of elasticity of 200,000 MPa and a strain-hardening ratio of 0.5% in beams and columns. Fiber sections were divided into smaller areas in the beams and columns. The net behavior was obtained by adding together the stress-strain responses

of the materials in these areas. The nonlinear effects of the members were also considered in modeling the beams and columns using a "*nonlinear beam-column element*", a widespread distribution of plasticity and seven integration points along each element. Moreover, buckling-restrained braces were modeled using the "*CorotTruss element*" with the same responses to compression and tension. In addition, nonlinear geometric effects were incorporated into the frame model using the geometric transformation of P-Δ. P-Δ effects were considered by linking leaning columns with gravity loads to the frame using rigid components.

To accurately determine the seismic behaviors of structures, nonlinear dynamic analyses were performed by exposing structures to actual ground motions, which were represented as temporal ground acceleration. Ground motions were recorded by determining this acceleration at small time steps. The design demand was then determined as the maximum value of the time history obtained by calculating the structural response at different moments. Moreover, the displacement and forces were obtained by subjecting a mathematical model that directly incorporates the nonlinear features of individual structural elements to earthquake shaking, which is represented as the time history of ground motions. The numerical models could accurately estimate the internal forces and inelastic responses that emerge during an earthquake by including the effect of material nonlinearity [62]. In this study, direct time integration method was used to provide time history analysis. $\gamma = 0.5$, $\beta = 0.25$ as Newmark parameters and 5% damping were considered for the Newmark method used for the time integration scheme. In addition, Maxwell's model has been used to apply nonlinear damping [63]. The present research evaluated the results of 96 nonlinear time history analyses.

## 3. Ground Motions

In the present research, 12 earthquake ground motions in far-field have been used to analyze the frames. The magnitudes of far-field earthquakes as high as 6.4–7.5 on the Richter scale were recorded at a distance of at least ten km from the fault in type 3 soil with a shear wave velocity of 175–375 m/s as per [23]. Hence, in this study, the real ground motion records were selected from the PEER-NGA database. The selected ground motions are generally characterized in Table 4.

**Table 4.** Ground Motion Records.

| Record | Earthquake | Station | PGA | M | Distance (km) |
|---|---|---|---|---|---|
| #EQ1 | Big Bear-1992 | Desert Hot Spr | 0.22 | 6.4 | 39.5 |
| #EQ2 | Imperial valley-06-1979 | Delta | 0.35 | 6.5 | 33.7 |
| #EQ3 | Imperial Valley-1979 | Calexico Fire Station | 0.277 | 6.5 | 10.45 |
| #EQ4 | Kobe_Japan-1995 | Shin Osaka | 0.233 | 6.9 | 46 |
| #EQ5 | Kocaeli_Turkey-1999 | Duzce | 0.36 | 7.5 | 98.2 |
| #EQ6 | Landers-1992 | North Palm Springs | 0.075 | 7.2 | 36.15 |
| #EQ7 | Landers-1992 | Yermo Fire Station | 0.2445 | 7.3 | 86 |
| #EQ8 | Loma Prieta-1989 | Gilroy Array #3 | 0.559 | 6.9 | 31.4 |
| #EQ9 | Loma Prieta-1989 | Coyote Lake Dam (Downst) | 0.18 | 7.1 | 20.8 |
| #EQ10 | Imperial valley-06-1979 | El Centro Array #11 | 0.379 | 6.5 | 29.4 |
| #EQ11 | Superstition Hills-02-1987 | El Centro Imp. Co | 0.357 | 6.5 | 35.8 |
| #EQ12 | Superstition Hills-1987 | Poe Road | 0.45 | 6.5 | 11.2 |

The average value of the square root of the sum of the squares of ground motions (SRSS) was set to at least equal 1.4 times the standard design threshold for periods of 0.2–1.5 T s, in which T represents the fundamental vibrational period [23]. The scaling process for the 10-story R-BRBF and the elastic response spectrum for the selected far-field ground motions with a damping of 5% are illustrated in Figure 3.

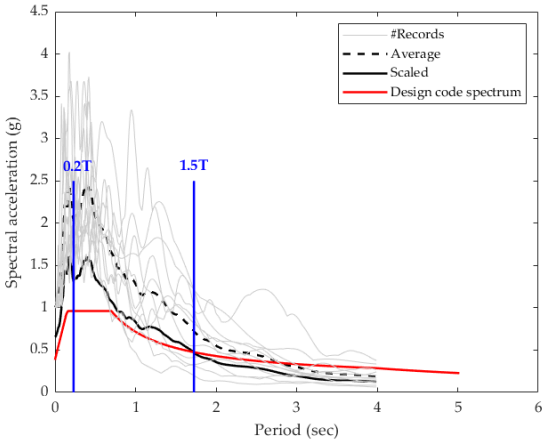


**Figure 3.** Process of scaling for the 10-story (R-BRBF).

## 4. Seismic Performance

### *4.1. Drift*

As a major step in the seismic design of structures, estimating and controlling of deformation increase the overall stability of buildings during earthquakes. Limiting the lateral displacement of a structure maintains its overall stability and prevents damage to its non-structural components such as mechanical equipment and architectural components. In this study, the maximum mean drift was observed in the irregular 10-and 15-story frames with mass irregularity BRBs under the effect of 12 far-field earthquakes. The minimum mean drift was recorded in the regular 10-and 15-story frames with regular CBFs. Using BRBs respectively increased the mean drift by 48% and 77% in the four irregular 10-story and four irregular 15-story frames compared to using CBFs, as shown in Figure 4. The Iranian code of practice for seismic resistant design of buildings [23] requires that the seismic drift be limited to 0.004 and 0.0057 in frames with BRBs and CBFs, respectively. Figure 4 compares the drift of the floors with its permissible value for both BRBFs and CBFs systems.

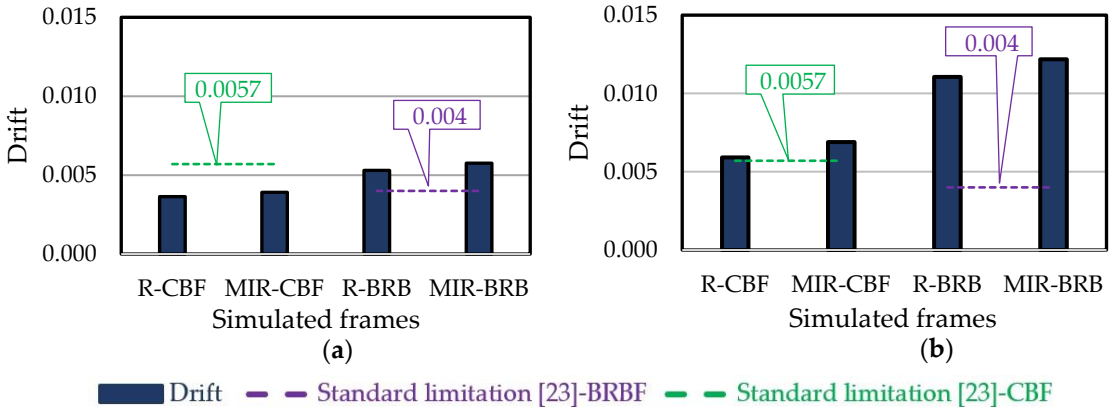


**Figure 4.** Average drift comparison of (**a**) 10-story frames and (**b**) 15-story frames.

Mass differences between two floors were found to insignificantly affect the average drift in the regular and irregular frames with the same lateral resisting system; for instance, the insignificant difference in the average drift between the regular (0.005) and irregular (0.006) 10-story frames with BRB (Figure 4) can be explained by the high stiffness of this kind of bracing. Two floors with different masses from their adjacent floors, one in the upper half and the other in the lower half of all the four irregular frames, imposed higher levels of inter-story drift on the intermediate floors and caused the damage to be concentrated in these floors, see Figure 5.

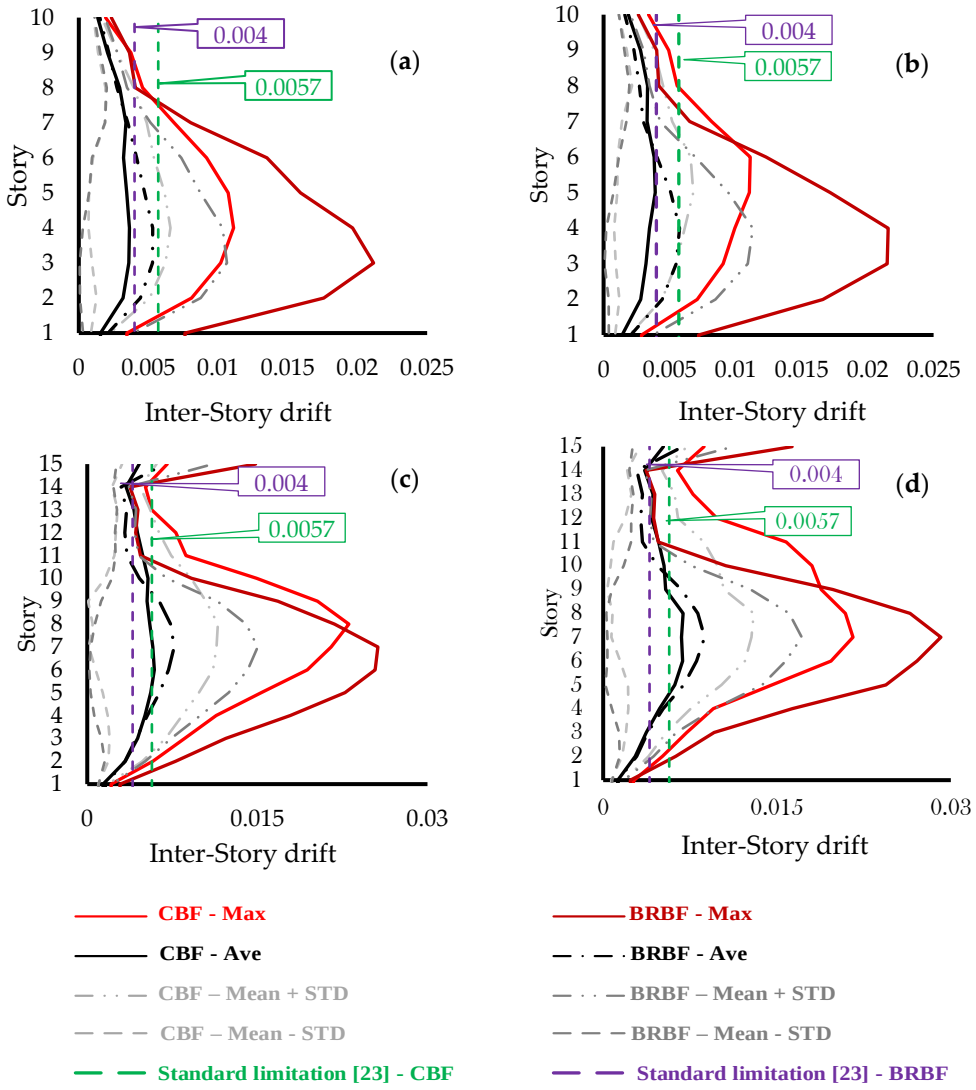


**Figure 5.** Inter-story drift of (**a**) 10-story regular frames, (**b**) 10-story mass irregularity frames, (**c**) 15-story regular frames and (**d**) 15-story mass irregularity frames.

In response to the #EQ5 (Duzce/Turkey Kocaeli) record, the maximum drift was observed in all the four types of the 10-story frames irrespective of their regularity or irregularity and type of bracing. This record was the highest in magnitude (7.5) among the 12 records selected in this study. According to Table 5, the maximum drift was equal to 0.022 in both the regular and irregular 10-story BRBFs and 0.011 in the regular and irregular 10-story CBF. In regular and irregular 10-story frames, the maximum drifts associated with BRBs were generally twice the maximum drift related to CBF. As in the 10-story frames, the maximum drift was observed in all the four types of 15-story frames under the effect of the #EQ5 (Duzce/Turkey Kocaeli) record. The maximum drift of the four types of the 15-story frames was higher in those with BRBs compared to in those with CBF irrespective of their regularity or irregularity (see Table 5).

**Table 5.** Maximum amount of seismic evaluation parameters.

| Type of Frames | Type of Response | | | | | | | | | | | | | | |
|---|---|---|---|---|---|---|---|---|---|---|---|---|---|---|---|
| | Drift | | | | Displacement (m) | | | | Base Shear (kN) | | | Acceleration (m/s$^2$) | | | |
| | Frame | Value | Event | story | Frame | Value | Event | story | Frame | Value | Event | Frame | Value | Event | story |
| 10-Story | R-CBF | 0.011 | Kocaeli | 4 | MIR-CBF | 0.181 | Kocaeli | 10 | R-CBF | 26,096 | Kocaeli | R-CBF | 7.665 | Gilroy | 10 |
| | MIR-CBF | 0.011 | Kocaeli | 5 | R-CBF | 0.183 | Kocaeli | 10 | MIR-CBF | 26,752.2 | Kocaeli | MIR-CBF | 7.579 | Gilroy | 10 |
| | R-BRB | 0.022 | Kocaeli | 3 | R-BRB | 0.317 | Kocaeli | 10 | R-BRB | 28,709.1 | Kocaeli | R-BRB | 7.506 | Gilroy | 10 |
| | MIR-BRB | 0.022 | Kocaeli | 4 | MIR-BRB | 0.322 | Kocaeli | 10 | MIR-BRB | 29,331.2 | Kocaeli | MIR-BRB | 7.877 | Gilroy | 10 |
| 15-Story | MIR-CBF | 0.022 | Kocaeli | 7 | R-CBF | 0.445 | Kocaeli | 15 | R-CBF | 10,862.1 | Shin-Osaka | R-CBF | 7.764 | Gilroy | 15 |
| | R-CBF | 0.023 | Kocaeli | 7 | MIR-CBF | 0.469 | Kocaeli | 15 | MIR-CBF | 26,908.8 | El centro Array | MIR-CBF | 8.458 | Gilroy | 15 |
| | R-BRB | 0.026 | Kocaeli | 7 | R-BRB | 0.500 | Kocaeli | 15 | R-BRB | 32,406 | Centro Imp. Co | R-BRB | 8.748 | Gilroy | 15 |
| | MIR-BRB | 0.029 | Kocaeli | 7 | MIR-BRB | 0.523 | Kocaeli | 15 | MIR-BRB | 34,582.4 | Centro Imp. Co | MIR-BRB | 9.141 | Gilroy | 15 |

It should be noted that, the permissible drift stipulated in the Iranian code of practice for seismic resistant design of buildings should be applied to the design of structures based on the equivalent static analysis, in which the first-mode effects are mostly considered. In contrast, the effects of higher modes, which are significant on high-rise buildings, were considered in the non-linear time history analysis of the structures. The present study compared the drift values of the 10-story and 15-story frames with the permissible drift of the seismic resistant design of buildings to show that the drift obtained from a non-linear dynamic analysis of the frames designed as per the equivalent static analysis might exceed the threshold in the code.

### *4.2. Displacement*

The mean displacement of the top floor was maximized in the irregular 10-and 15-story frames with mass irregularity BRBs and minimized in the regular frames with regular CBFs. In the irregular 10-and 15-story frames, using mass irregularity BRBs respectively increased the displacement by 30% and 7% compared to using mass irregularity CBFs, as shown in Figures 6 and 7. Both the regular and irregular frames with CBFs thus outperformed those with BRBs in terms of the top floor displacement.

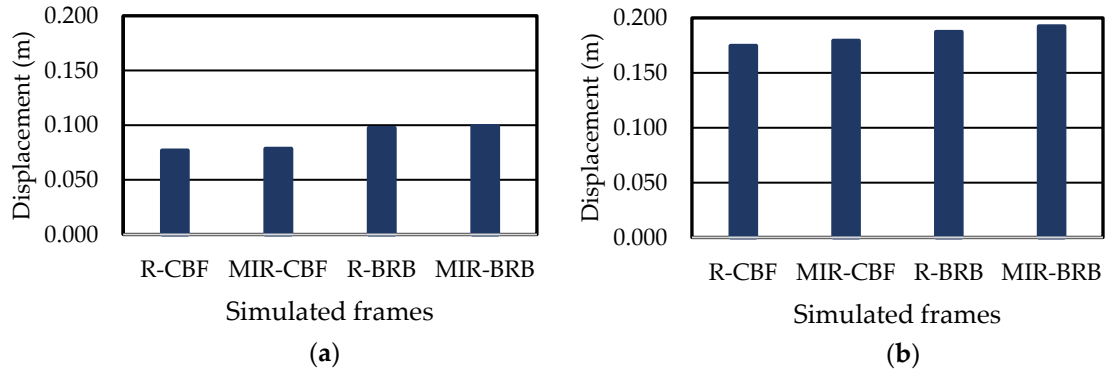


**Figure 6.** Average displacement comparison of (**a**) 10-story frames and (**b**) 15-story frames.

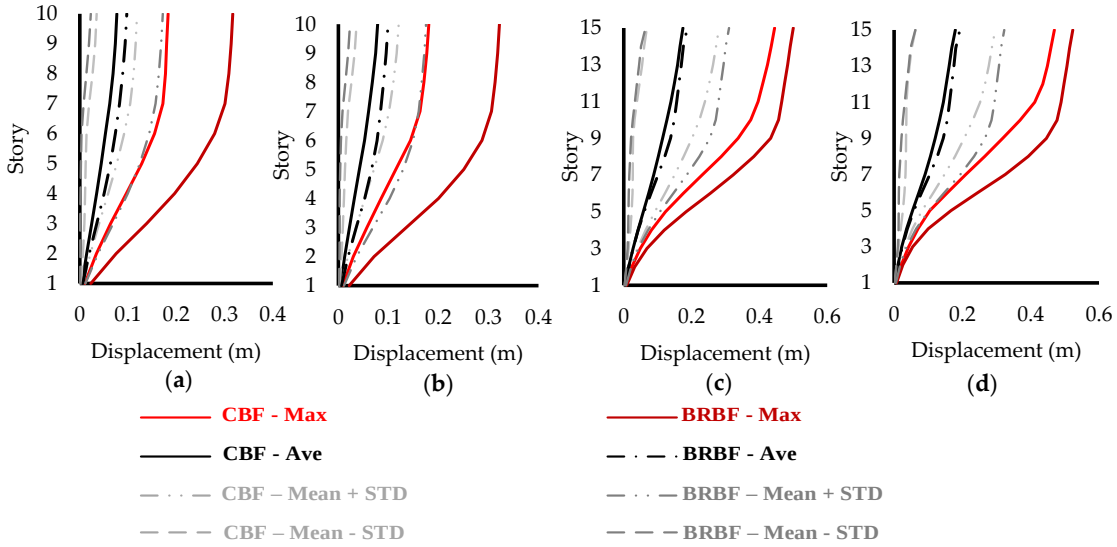


**Figure 7.** Displacement of (**a**) 10-story regular frames, (**b**) 10-story mass irregularity frames, (**c**) 15-story regular frames and (**d**) 15-story mass irregularity frames.

The displacement of the top floors was higher in the 10-story and 15-story BRBFs compared to in those with CBFs. The maximum displacement observed in all the eight frames under the effect of the #EQ5 (Duzce/Turkey Kocaeli) record was higher in the 15-story frames of the four types than in the

10-story frames of the corresponding type. Moreover, the maximum displacement was higher in the irregular than regular 15-story CBFs or BRBFs, see Table 5.

### *4.3. Base Shear*

Structural engineers use the base shear as a key parameter in the design of structures. Investigating the behavior of the 10-story frames showed that the mean base shear was the highest in the regular frames with regular CBFs, the lowest in the irregular frames with mass irregularity BRBs and approximately equal in the regular and irregular frames with the same type of brace. In other words, the mean base shear was not significantly affected by the frame regularity. Investigating the 15-story frames showed the highest observed base shear in the frames with mass irregularity BRBs (see Figure 8).

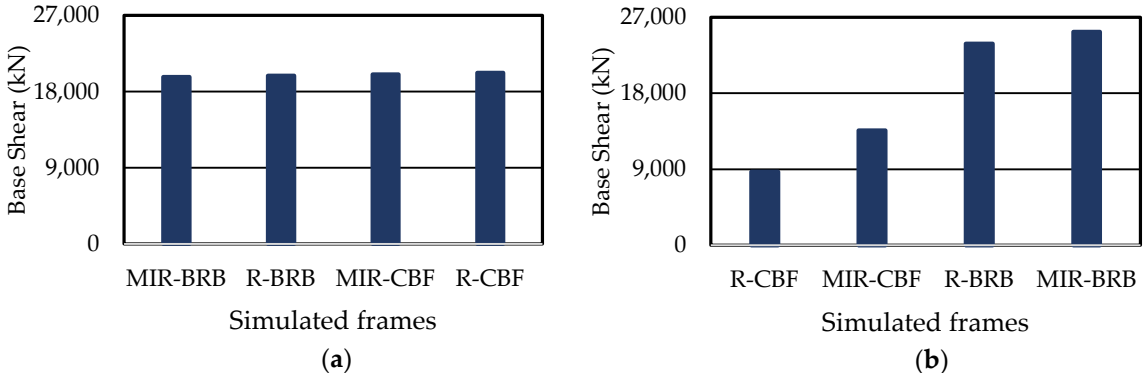


**Figure 8.** Average base shear comparison of (**a**) 10-story frames and (**b**) 15-story frames.

The maximum base shear was reported under the effect of the #EQ5 (Duzce/Turkey Kocaeli) record in the MIR-BRBF among the four 10-story frames. The maximum base shear was, however, reported under the effect of #EQ11 (El Centro Imp. Co California/USA Superstition Hills) in the 15-story MIR-BRBF. Table 5 shows the amount of maximum base shear related to each frame.

### *4.4. Acceleration*

This study examined the floor acceleration as a fundamental parameter in designing non-structural components, as shown in Figure 9. The maximum acceleration was recorded in the top floors of both the 10-and 15-story frames under the effect of #EQ8 (Gilroy Array #3 California/USA Loma Prieta). Comparing the mean values of the maximum acceleration of the 10-story frames showed negligible differences among these values. Irrespective of the number of floors, the highest and lowest values of the mean acceleration were respectively associated with the frames with mass irregularity BRBs and regular CBFs. Reductions in the floor acceleration caused by CBFs were higher than those caused by BRBFs.

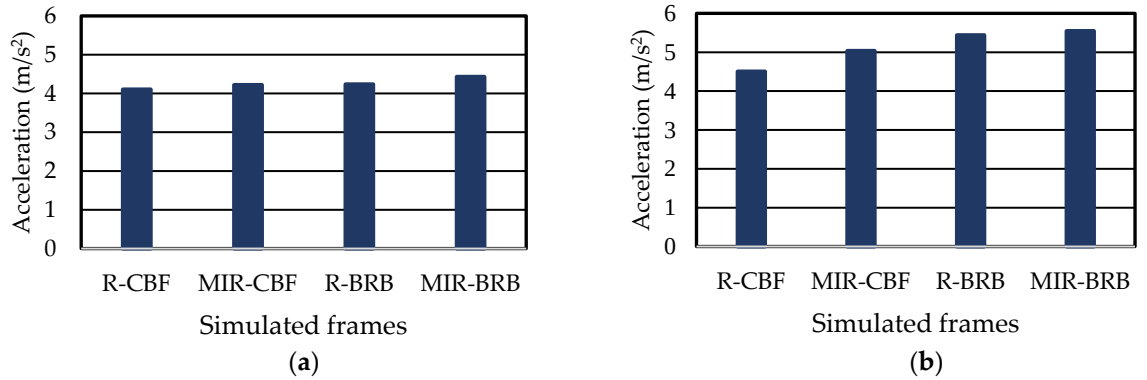


**Figure 9.** Average acceleration comparison of (**a**) 10-story frames and (**b**) 15-story frames.

With the highest PGA (0.55) among the 12 selected records, the Gilroy Array #3 record imposed the highest acceleration on the top floors of all the eight frames. Irrespective of the number of floors, the maximum acceleration was reported in the MIR-BRB. Amounts of maximum acceleration are illustrated in Table 5.

## 5. Conclusions

Architecture and application of a structure play a major role in its seismic behavior. Today, given the limited available land and its high price in densely populated cities, structural designers have no choice but to design structures with irregularities in the plan and height. An accurate engineering judgement of the complicated behavior of irregular buildings during earthquakes plays a key role in improving the design quality of these structures. This study evaluated the seismic responses of eight regular and irregular 10- and 15-story CBF and BRB frames using the records of 12 far-field earthquakes. According to classification of HAZUS-MH MR5 [59] regulation, 10- and 15-story buildings are considered as high-rise buildings. The following results are obtained by undertaking nonlinear time-history analysis for modeling the frames:

- Based on the results of the nonlinear time history analyses, regardless of the regularity status of the frames, the mean drift is lower in the CBFs than BRBFs. In other words, the CBFs improve the drift performance in comparison with the BRBFs. Compared to using CBFs, employing the BRBFs increase the mean drift by 47% and 77% in the irregular 10-story and 15-story frames, respectively. Furthermore, the maximum drift is higher in the frames with BRBs than in those with CBFs irrespective of their number of floors and regularity. With the largest magnitude among the 12 selected records, Duzce earthquake (Kocaeli, Turkey) also imposes the highest drift on all the eight studied frames.
- In contrast to the 10-story frames, using the BRB increase the base shear as a design parameter in both the regular and irregular 15-story frames. Moreover, the maximum base shear is observed in the 10-and 15-story MIR-BRBF.
- Negligible differences are ultimately observed in the mean value of the maximum floor acceleration between the four regular and irregular 10-story frames with either CBFs or BRBs. In contrast, the mean value of the maximum acceleration is higher in the 15-story frames with BRBs than in those with CBFs.
- An earthquake with the highest PGA among all the selected records imposes the highest acceleration on the top floors of all the eight frames. The maximum acceleration is also reported in the 10- and 15-story MIR-BRBFs.
- The maximum displacement of the top floor is higher in the frames with BRBs than in those with CBFs.

**Author Contributions:** Conceptualization, A.K. and S.S.; methodology, A.K. and S.S.; software, A.K.; formal analysis, S.S.; investigation, M.K.; data curation, M.K.; writing—original draft preparation, A.K. and S.S.; writing—review and editing, S.S., M.K. and A.K.; supervision, M.K. All authors have read and agreed to the published version of the manuscript.

**Funding:** This research received no external funding.

**Conflicts of Interest:** The authors declare no conflict of interest.

## References

1. Takeuchi, T.; Wada, A. Review of Buckling-Restrained Brace Design and Application to Tall Buildings. *Int. J. High-Rise Build.* **2018**, *7*, 187–195. [CrossRef]
2. Takeuchi, T.; Wada, A. *Buckling-Restrained Braces and Applications*; JSSI: Tokyo, Japan, 2017.
3. Kim, D.H.; Lee, C.H.; Ju, Y.K.; Kim, S.D. Sub assemblage test of buckling-restrained braces with H-shaped steel core. *Struct. Des. Tall Spec. Build.* **2015**, *24*, 243–256. [CrossRef]

4. Lai, M.H.; Chen, M.T.; Ren, F.M.; Ho, J.C.M. Uni-axial behavior of externally confined UHSCFST columns. *Thin Walled Struct.* **2019**, *142*, 19–36. [CrossRef]
5. Kioumarsi, B.; Kheyroddin, A.; Gholhaki, M.; Kioumarsi, M.; Hooshmandi, S. Effect of span length on behavior of MRF accompanied with CBF and MBF systems. *Procedia Eng.* **2017**, *171*, 1332–1340. [CrossRef]
6. Bypour, M.; Gholhaki, M.; Kioumarsi, M.; Kioumarsi, B. Nonlinear analysis to investigate effect of connection type on behavior of steel plate shear wall in RC frame. *Eng. Struct.* **2019**, *179*, 611–624. [CrossRef]
7. Kioumarsi, B.; Gholhaki, M.; Kheyroddin, A.; Kioumarsi, M. Analytical study of building height effects over Steel Plate Shear Wall Behavior. *Int. J. Eng. Technol. Innov.* **2016**, *6*, 255–263.
8. Bypour, M.; Kioumarsi, M.; Yekrangnia, M. Shear capacity prediction of stiffened steel plate shear walls (SSPSW) with openings using response surface method. *Eng. Struct.* **2021**, *226*, 111340. [CrossRef]
9. Bypour, M.; Kioumarsi, B.; Kioumarsi, M. Investigation of Failure Mechanism of Thin Steel Plate Shear Wall in RC Frame. *Key Eng. Mater.* **2019**, *803*, 314–321. [CrossRef]
10. Vafaei, D.; Eskandari, R. Seismic response of mega buckling-restrained braces subjected to fling-step and forward-directivity near-fault ground motions. *Struct Des. Tall Spec. Build.* **2015**, *24*, 672–686. [CrossRef]
11. Liu, X.; Zhou, X.; Zhang, A.; Tian, C.; Zhang, X.; Tan, Y. Design and compilation of specifications for a modular-prefabricated high-rise steel frame structure with diagonal braces. Part I: Integral structural design. *Struct. Des. Tall Spec. Build.* **2018**, *27*, e1415. [CrossRef]
12. Nazarimofrad, E.; Shokrgozar, A. Seismic performance of steel braced frames with self-centering buckling-restrained brace utilizing super elastic shape memory alloys. *Struct. Des. Tall Spec. Build.* **2019**, *28*, e1666. [CrossRef]
13. Chou, C.C.; Hsiao, C.H.; Chen, Z.B.; Chung, P.T.; Pham, D.H. Seismic loading tests of full-scale two-story steel building frames with self-centering braces and buckling-restrained braces. *Thin-Walled Struct.* **2019**, *140*, 168–181. [CrossRef]
14. Lin, P.; Takeuchi, T.; Matsui, R. Seismic performance evaluation of single damped outrigger system incorporating buckling-restrained braces. *Earthq. Eng. Struct. Dyn.* **2018**, *47*, 2343–2365. [CrossRef]
15. Xing, L.; Zhou, Y. Optimization analysis of ordinary outrigger trusses and outrigger trusses with buckling restrained braces. *J. Build. Struct.* **2018**, *36*, 1–10. (In Chinese) [CrossRef]
16. Beiraghi, H. Near-fault ground motion effects on the responses of tall reinforced concrete walls with buckling-restrained brace outriggers. *Sci. Iran.* **2018**, *25*, 1987–1999. [CrossRef]
17. Deng, K.; Pan, P.; Lam, A.; Xue, Y. A simplified model for analysis of high-rise buildings equipped with hysteresis damped outriggers. *Struct. Des. Tall Spec. Build.* **2014**, *23*, 1158–1170. [CrossRef]
18. Lin, P.C.; Takeuchi, T.; Matsui, R. Optimal design of multiple damped-outrigger system incorporating buckling-restrained braces. *Eng. Struct.* **2019**, *194*, 441–457. [CrossRef]
19. Asai, T.; Chang, C.M.; Phillips, B.M.; Spencer, B.F., Jr. Real-time hybrid simulation of a smart outrigger damping system for high-rise buildings. *Eng. Struct.* **2013**, *57*, 177–188. [CrossRef]
20. Xinga, L.; Zhoua, Y.; Huang, W. Seismic optimization analysis of high-rise buildings with a buckling restrained brace outrigger system. *Eng. Struct.* **2020**, *220*, 110959. [CrossRef]
21. Zhou, Y.; Zhang, C.Q.; Lu, X.L. Seismic performance of a damping outrigger system for tall buildings. *Struct. Control Health Monit.* **2017**, *24*, e1864. [CrossRef]
22. Darshan, D.; Shruthi, H.K. Study on Mas Irregularity of High-Rise Buildings. *Int. Res. J. Eng. Technol. (Irjet)* **2016**, *3*, 1123–1131.
23. Standard 2800. *Iranian Code of Practice for Seismic Resistant Design of Buildings*, 4th ed.; Building and Housing Research Center: Tehran, Iran, 2014.
24. Pirizadeh, M.; Shakib, H. Probabilistic seismic performance evaluation of non-geometric vertically irregular steel buildings. *J. Constr. Steel Res.* **2013**, *82*, 88–98. [CrossRef]
25. Shakib, H.; Nodeh, M.; Homaei, F. Fragility Curve Development for Assessing Midrise Steel Building with Buckling Resistant Braced System Having Vertical Irregularity. *JSEE* **2015**, *17*, 293–304.
26. Amiri, M.; Yakhchalian, M. Performance of intensity measures for seismic collapse assessment of structures with vertical mass irregularity. *Structures* **2020**, *24*, 728–741. [CrossRef]
27. Naveen, E.S.; Abraham, N.M.; Kumari, D.A. Parametric Studies on the Seismic Behavior of Irregular Structures. *Struct. Integr. Assess.* **2019**, *48*, 839–850. [CrossRef]
28. Angelos, S.T.; Konstantinos, A.S.; Beskos, D.E. A Hybrid Seismic Design Method for Steel Irregular Space Moment Resisting Frames. *J. Earthq. Eng.* **2020**, 1–36. [CrossRef]

29. Köber, D. Seismic Design Particularities of a Five Story Reinforced Concrete Structure, Irregular in Plan and Elevation. In *Seismic Behaviour and Design of Irregular and Complex Civil Structures III*; Springer: Cham, Switzerland, 2020; pp. 189–199. [CrossRef]
30. Yassin, A. Seismic Performance Evaluation of Stiffness Irregular RC Buildings due to Story Height Difference. Master's Thesis, Science in Civil Engineering, Addis Ababa Science and Technology University, Addis Ababa, Ethiopia, October 2019.
31. Ngamkhanong, C.; Kaewunruen, S.; Baniotopoulos, C. Far-Field Earthquake Responses of Overhead Line Equipment (OHLE) Structure Considering Soil-Structure Interaction. *Front. Built Environ.* **2018**, *4*, 35. [CrossRef]
32. Chen, R.; Qiu, C.; Hao, D. Seismic Response Analysis of Multi-Story Steel Frames Using BRB and SCB Hybrid Bracing System. *Appl. Sci.* **2020**, *10*, 284. [CrossRef]
33. Shen, J.; Seker, O.; Akbas, B.; Seker, P.; Momenzadeh, S.; Faytarouni, M. Seismic performance of concentrically braced frames with and without brace buckling. *Eng. Struct.* **2017**, *141*, 461–481. [CrossRef]
34. Hsiao, P.C.; Lehman, D.E.; Roeder, C.W. Improved analytical model for special concentrically braced frames. *J. Constr. Steel Res.* **2012**, *73*, 80–94. [CrossRef]
35. Hoveidae, N.; Rafezy, B. Overall buckling behavior of all-steel buckling restrained braces. *J. Constr. Steel Res.* **2012**, *79*, 151–158. [CrossRef]
36. Hosseinzadeh, S.H.; Mohebi, B. Seismic evaluation of all-steel buckling restrained braces using finite element analysis. *J. Constr. Steel Res.* **2016**, *119*, 76–84. [CrossRef]
37. Zhu, B.L.; Guo, Y.L.; Zhou, P.; Bradford, M.A.; Pi, Y.L. Numerical and experimental studies of corrugated-web-connected buckling-restrained braces. *Eng. Struct.* **2017**, *134*, 107–124. [CrossRef]
38. Ebadi Jamkhaneh, M.; Kafi, M.A. Equalizing octagonal PEC columns with steel columns: Experimental and theoretical study. *Pract. Period. Struct. Des. Constr.* **2018**, *23*, 04018012. [CrossRef]
39. Ebadi Jamkhaneh, M.; Kafi, M.A. Experimental and numerical study of octagonal composite column subject to various loading. *Period. Polytech. Civ. Eng.* **2018**, *62*, 413–422. [CrossRef]
40. Ahadi Koloo, F.; Badakhshan, A.; Fallahnejad, H.; Ebadi Jamkhaneh, M.; Ahmadi, M. Investigation of proposed concrete filled steel tube connections under reversed cyclic loading. *Int. J. Steel Struct.* **2018**, *18*, 163–177. [CrossRef]
41. Ebadi Jamkhaneh, M.; Homaioon Ebrahimi, A.; Shokri Amiri, M. Investigation of the Seismic Behavior of Brace Frames with New Corrugated All-Steel Buckling Restrained Brace. *Int. J. Steel Struct.* **2019**, *19*, 1225–1236. [CrossRef]
42. Karavasilis, T.L.; Bazeos, N.; Beskos, D.E. Estimation of seismic inelastic deformation demands in plane steel MRF with vertical mass irregularities. *Eng. Struct.* **2008**, *30*, 3265–3275. [CrossRef]
43. Valmundsson, E.V.; Nau, J.M. Seismic response of building frames with vertical structural irregularities. *J. Struct. Eng.* **1997**, *123*, 30–41. [CrossRef]
44. Choi, B.J. Hysteretic energy response of steel moment-resisting frames with vertical mass irregularities. *Struct. Des. Tall Spec. Build.* **2004**, *13*, 123–144. [CrossRef]
45. ASCE/SEI 7-16. *Minimum Design Loads for Buildings and other Structures*; SEI: Reston, VA, USA, 2017.
46. Davoodi, M.; Sadjadi, M. Assessment of near-field and far-field strong ground motion effects on soil-structure SDOF system. *IJCE* **2015**, *13*, 153–166. [CrossRef]
47. Ngamkhanong, C.; Pinkaew, T. Effectiveness of tuned mass damper in damage reduction of building under far-field ground motions. In Proceedings of the 5th ECCOMAS Thematic Conference on Computational Methods in Structural Dynamics and Earthquake Engineering (Crete), Crete Island, Greece, 25–27 May 2015; pp. 972–983. [CrossRef]
48. Ansari, M.; Safiey, A. Evaluation of seismic performance of mid-rise reinforced concrete frames subjected to far-field and near field ground motions. *Earthq. Struct. Struct.* **2018**, *5*, 453–462. [CrossRef]
49. Mortezaei, A.; Ronagh, H.R. Plastic hinge length of reinforced concrete columns subjected to both far fault and near fault ground motions having forward directivity. *Struct. Des. Tall Spec. Build.* **2013**, *22*, 903–926. [CrossRef]
50. Cao, V.V.; Ronagh, H.R. Correlation between seismic parameters of far-fault motions and damage indices of low-rise reinforced concrete frames. *Soil Dyn. Earthq. Eng.* **2014**, *66*, 102–112. [CrossRef]
51. Zhang, S.; Wang, G. Effects of near-fault and far-fault ground motions on nonlinear dynamic response and seismic damage of concrete gravity dams. *Soil Dyn. Earthq. Eng.* **2013**, *53*, 217–229. [CrossRef]

52. Belejo, A.; Bento, R. Improved modal pushover analysis in seismic assessment of asymmetric plan buildings under the influence of one and two horizontal components of ground motions. *Soil Dyn. Earthq. Eng.* **2016**, *87*, 1–15. [CrossRef]
53. Balic, I.; Trogrlic, B.; Mihanovic, A. Simplified multimodal pushover target acceleration method for seismic resistance analysis of medium-rise RC structures. *KSCE J. Civ. Eng.* **2017**, *21*, 378–388. [CrossRef]
54. Li, S.; Zuo, Z.; Zhai, C.; Xie, L. Comparison of static pushover and dynamic analyses using RC building shaking table experiment. *Eng. Struct.* **2017**, *136*, 430–440. [CrossRef]
55. Shahbazi, S.H.; Karami, A.; Mansouri, I.; Hu, J.W. Seismic response of steel moment frames (SMFs) considering simultaneous excitations of vertical and horizontal components, including fling-step ground motions. *Appl. Sci.* **2019**, *9*, 2079. [CrossRef]
56. Shahbazi, S.H.; Mansouri, I.; Hu, J.W.; Sam Daliri, N.; Karami, A. Seismic response of steel SMFs subjected to vertical components of far-and near-field earthquakes with forward directivity effects. *Adv. Civ. Eng.* textbf2019. [CrossRef]
57. Mansouri, I.; Shahbazi, S.; Nejat, M.; Karami, A. Effect of Soil Classification on Seismic Behavior of SMFs considering Soil-Structure Interaction and Near-Field Earthquakes. *Shock Vib.* **2018**. [CrossRef]
58. Shahbazi, S.; Khatibinia, M.; Mansouri, I.; Hu, J.W. Seismic evaluation of special steel moment frames undergoing near-field earthquakes with forward directivity by considering soil-structure interaction effects. *Sci. Iran.* **2018**. [CrossRef]
59. Mansouri, I.; Shahbazi, S.; Hu, J.W.; Moghaddam, S.A. Effects of pulse-like nature of forward directivity ground motions on the seismic behavior of steel moment frames. *Earthq. Struct.* **2019**, *17*, 1–15. [CrossRef]
60. HAZUS-MH MR5: Multi-Hazard Loss Estimation Methodology: Earthquake Model. In *Federal Emergency Management Agency*; U.S. Department of Homeland Security: Washington, DC, USA, 2011.
61. ACI Committee 318. *Building Code Requirements for Structural Concrete (ACI 318-05) and Commentary (ACI 318R-05)*; American Concrete Institute: Farmington Hills, MI, USA, 2005.
62. Shaik, I.; Anwar, S.F.; Hashmath, M. Response Spectrum and Time History Analysis of a Multistoried and Commercial Building. *Glob. J. Eng. Sci. Res.* **2017**, 4. [CrossRef]
63. Mazzoni, S.; McKenna, F.; Scott, M.H.; Fenves, G.L. *OpenSees Command Language Manual*; University of California: Berkeley, CA, USA, 2006; Available online: http://opensees.berkeley.edu/manuals/usermanual (accessed on 19 July 2006).